TRANSITION TO PERIODIC UNSTEADY AND EFFECTS OF PRANDTL NUMBERS ON THE FLOW ACROSS A CONFINED HEATED TRAPEZOIDAL BLUFF BODY

A DISSERTATION

Submitted in Partial fulfillment of the requirement for the award of the degree

of

MASTER OF TECHNOLOGY

in

CHEMICAL ENGINEERING

(with specialization in computer aided process plant design)

By

MALIK PARVEEZ

DEPARTMENT OF CHEMICAL ENGINEERING

INDIAN INSTITUTE OF TECHNOLOGY ROORKEE

ROORKEE -247 667 (INDIA)

MAY, 2014

Declaration

I hereby declare that the work presented in this dissertation entitled " **Transition to periodic unsteady and effects of Prandtl numbers on the flow across a confined heated trapezoidal bluff body"** submitted towards partial fulfillment for the award of the degree of M.Tech in chemical Engineering with specialization in computer Aided process plant Design at the Indian Institute of Technology, Roorkee is reliable record of my original work conceded under the guidance of **DR. A. K. Dhiman** (IIT Roorkee). I have not submitted the matter embodied in this dissertation for the award of any degree.

Place:- Roorkee Malik Parveez

Date:- 02/05/2014

Certificate

This is to certify that Mr. Malik Parveez (Enrol. No. 12514008) has completed the dissertation entitled " **Transition to periodic unsteady and effects of Prandtl numbers on the flow across a confined heated trapezoidal bluff body"** under my supervision.

(Dr.A. K. Dhiman)
Associate Professor
Department of Chemical Engineering
IIT Roorkee

ACKNOWLEDGEMENTS

First and foremost, I am indebted to my almighty God, the architect and the Guardian and to whom I be obligated my very existence.

It is with great affection and admiration that I acknowledge my indebtedness to Dr. Amit Kumar Dhiman, Associate Professor, Department of Chemical Engineering, Indian Institute of Technology-Roorkee, who has supported me throughout my work with his patience, knowledge and friendly attitude. I greatly acknowledge his suggestion, direction and crucial contribution, which made him the honorable character of this research. I wish to express my thanks to Dr. V.K. Agrawal, Professor & Head, Chemical Engineering Department, IIT-Roorkee who allowed me to use the departmental computing facility for executing my research work. This would have not been possible without the tolerance of my family especially my son Malik Essa and daughter Malik Hanaa. My wife Huma Malik deserves particular mention for her inseparable support. My dad Malik Zulfikar and mom Shameem are the one who raised me with caring, unconditional love and prayers. My gratitude to my lab-mates Deepak kumar, Ram Pravesh, Manusukasan, Tanveer Rasool, Vivek verma and Anirudha saniyal for creating learning atmosphere in lab. and also providing valuable suggestions and help as and when required to work in. I would like to thank all the teaching and non-teaching staff of Chemical Engineering for making my two years of M.Tech. a truly inspirational educational experience.

Malik Parveez

En. no 12514008

M-Tech. (C.A.P.P.D)

Topic	Table of contents	Page No.

Abstract

Effects of wall confinements (β) and of Prandtl numbers (Pr) on the two-dimensional laminar flow around a heated tapered trapezoidal bluff body are investigated numerically at low Reynolds numbers (Re) for $0.71 \leq Pr \leq 100$ and $12.5\% \leq \beta \leq 50\%$. The critical Reynolds number (i.e. the switch from a steady to a time-periodic flow) is calculated and it exists between Re = (36 and 37), (60 and 61) and (91 and 92) for β of 12.5%, 25% and 50%, respectively. The $\bar{Nu}$ (average) increases with the increasing value of Re and/or Pr and/or β. The variation of Nu (local) on each surface of the cylinder and the isotherm contours are presented to clarify the role of Prandtl number and β on transfer of heat from the trapezoidal bluff body. The maximum heat transfer enhancement with respect to a square bluff body on the basis of equal projected area is found to be approximately 31% and 45% for β = 12.5% and 25%, and for Pr=0.71 and Re=1. Finally, the Colburn heat transfer factor correlations are obtained for the preceding range of settings.

***Keywords*:** Trapezoidal bluff body; Blockage ratio; Critical Reynolds number; Prandtl number; Nusselt number; the Colburn heat transfer factor and Heat transfer enhancement.

Nomenclature

a	downstream side of a tapered trapezoidal obstacle, m
b	upstream side of a tapered trapezoidal obstacle, m
C_L	total lift coefficient ($=F_L /(0.5\rho U^2_\infty b)$)
c_p	fluid specific heat, J $kg^{-1}K^{-1}$
f	vortex shedding frequency, s^{-1}
h	heat transfer coefficient (local), W m^{-2} K^{-1}
$\bar{h}$	heat transfer coefficient (average), W m^{-2} K^{-1}
H	domain height, m
j_h	the Colburn heat transfer factor
k	conductivity (thermal) , W m^{-1} K^{-1}
L	domain length, m
Lr	recirculation distance, m
Nu	Nusselt number (local) ($= h\mathrm{b}/k$)
$\bar{Nu}$	Nusselt number (average) ($= \bar{h}\mathrm{b}/k$)
Pr	Prandtl number ($= \mu c_p / k$)
Re	Reynolds number ($= \rho U_\infty \mathrm{b} / \mu$)
Re_c	critical Reynolds number
St	Strouhal number ($=fb/U_\infty$)
T^*	temperature, K
T_∞	fluid temperature at the inlet, K
T^*_w	wall temperature (constant) at the face of the cylinder, K

U_∞	inlet velocity (avg.), m s^{-1}
V_x	component of the velocity in the *x*- direction ($=V_x^*/U_\infty$)
V_y	component of the velocity in the *y*- direction ($=V_y^*/U_\infty$)
X_d	distance from rear end of cylinder to exit, m
X_u	distance from inlet to front end of cylinder, m

Greek symbols

β	($=b/H$)
θ	($=(T^*-T_\infty)/(T_w^*-T_\infty)$)
μ	fluid viscosity, kg m^{-1} s^{-1}
ρ	fluid density, kg m^{-3}

Subscript

c	critical value
w	surface of the trapezoidal cylinder
∞	inlet condition

Superscript

*	dimensional variable

List of Publications

International Journals:

1. M. Parveez , A. Dhiman, T. Rasool, Transition to periodic unsteady and effects of Prandtl numbers on the flow across a confined heated trapezoidal bluff body, Brazilian Journal of Chemical Engineering (under review).

Conferences:

1. M. Parveez , A. Dhiman, T. Rasool , Confined momentum and heat transfer phenomena around a bluff body of trapezoidal cross-section, Proceedings of the National conferences on Innovations and development in Chemical Technology Feb. 28-01-2014, GGIPU, Dawarka Delhi.

CHAPTER 1: Introduction

The flow around a bluff body has been comprehensively investigated numerically as well as experimentally due to its pragmatic implications e.g design of heat exchange systems, designing of oil buoys and floating structures, probes and flow measuring devices. Flow of a fluid past a trapezoidal shape bluff body is more complicated phenomenon than that observed around a circular cylinder. For instance, the industrial flow meters utilize the relation between the shedding frequency and the flow rate or velocity, a trapezoidal shape is found to be more advantageous than a circular cylinder **[1]**. Besides the Reynolds number, the vortex shedding depends strongly on the wall confinement. The parameters like C_D (drag coff.), Lr (recirculation length) etc show dependence on Re (Reynolds number) and Pr (Prandtl number). This work has been taken to elucidate transition to periodic unsteady and effects of Prandtl numbers on the flow across a confined heated trapezoidal bluff body, also the role of β (blockage) on the streamlines and heat flow pattern as well. The continuity (mass), Navier-Stokes and energy equations are solved by using a finite volume solver Ansys Fluent.

In order to understand the phenomenon properly a few terms are needed to be addressed in details which are as follows.

1.1 Bluff body flow

. A boundary layer separation is always practiced by a bluff body when a fluid flows past it. If the face facing the flow have sufficient cross section, as a result, change the flow pattern it is called bluff body. Flow over a moving track or car or wind moving along skyscrapers are some examples of bluff-body flow. There exist a region behind the bluff body where the flow is slowed down. It creates an unsteady, which makes the bluff body vibrate and may lead to structural failure, especially when the frequency of shedding matches one of the resonant frequencies of the structure. A famous incident happens in history called Tacoma bridge collapse. A boundary layer separation is always practiced by a bluff body when a fluid flows past it. Behind this bluff body as here it is considered tapered trapezoidal, a periodic flow motion will build up in the wake because of boundary layer vortex shedding from either side of the cylinder at certain range of Reynolds number.

1.2 Flow separation: When the fast moving vehicle jumps over hills the separation of wheels takes place from the surface but if the vehicle moves with low speed no separation takes place. Same phenomena is observed when the moving fluid pass the curved surface. It is very difficult to predict where the separation will takes place and this point of separation depends on Reynolds number, surface roughness etc. Due to flow separation, it results in the formation of circulating fluid region which is just adjacent to the back side of the body called as vortices.

1.2 Wake: The re-circulating flow formed behind a moving or stationary solid body, called as wake caused by the flow of surrounding fluid around the body. In fluid dynamics terminology a wake is the region of disturbed flow (usually turbulent) on the posterior side of a solid body moving through a fluid, caused by the flow of the fluid around the body. The pressure is found to be maximum at the point where the fluid is stagnant and decrease along the front half of the cylinder. As the flow reaches the posterior end, the pressure start to built on that side of the cylinder and ultimately results in adverse pressure gradient. As a result, the flow separates from the surface and creating a highly disturbed zone behind the cylinder called the wake.

1.4 Vortex shedding: A shear layer which is highly disturbed separates from the surface of the bluff body. This shear layer turns round and finally form an isolated vortex and the phenomena is called vortex shedding. Also this shear layer separates from the top and bottom surface alternatively and eventually interact with each other forming a regular vortex pattern called as Karaman vortex street. The frequency at which vortexes are formed depend on various parameters like shape of bluff body but Reynolds number play a vital role in vortex shedding.

1.5. Drag and lift

Force exerted by a flowing fluid in the direction of flow on a body is called drag. when the body is immersed in stationary fluid, normal pressure force gets exerted on the surface of body. Tangential shear force is exerted on the surface of the body because of no-slip conditions and it only occurs when the fluid is moving and because of effects of viscosity. while as normal pressure force acts on the surface of body immersed in stationary fluid. Thus in general, drag force is due to the mutual effects of pressure and wall shear force in the direction of flow. The body moves in the direction normal to flow when the components of the pressure and wall shear

forces acts in the directions normal to the flow and their sum is called lift. Thus for 2-D flows, the resultant of the pressure and wall shear forces can be resolved into two components, one is the drag force that is in the direction of flow, and the another which normal to flow which is the lift. These force are related with the density ρ of the fluid, the velocity V, and the size, shape, and the body orientation. It is more appropriate to work dimensionless numbers that represent the drag and lift characteristics of the body. These numbers are drag coefficient C_D and lift coefficient C_L and are defined as

$$C_D = \frac{F_D}{\frac{1}{2}\rho V^2 A}$$

$$C_L = \frac{F_L}{\frac{1}{2}\rho V^2 A}$$

1.6. Dimensional Groups:

The simple scaling and dimensional considerations of this flow suggest the following dimensionless numbers is used to characterize the flow.

1.6.1 Reynolds Number (Re)

The Reynolds number is obtained by considering the ratio of inertial force and viscous force. The definitions of this dimensionless number include the fluid properties like density and viscosity, also a velocity and length as (characteristics dimension). Reynolds number is generally defined as:

$Re=\rho v D_H/\mu = vDH/\upsilon = QDH/\upsilon A$

D_H= diameter of pipe (hydraulic), length is L(m), Q= flow rate (m^3/s), A= cross-sectional area of pipe (m^2), V= velocity (mean) (m/s), μ= viscosity (dynamic) of fluid (pa-s), υ= kinematic viscosity (m^2/s), ρ=density of fluid (m^3/s)

1.6.2.Prandtl number (Pr)

It is expressed as the ratio of momentum diffusivity (kinematic viscosity) and thermal diffusivity.

Pr =μCp/k = υ/α =viscous diffusion rate/Thermal diffusion rate, υ= viscosity (kinematic) = μ/ρ (m^2/s), α = diffusivity (thermal) = (k/ρCp) (m^2/s), μ = dynamic viscosity (pa-s), k = conductivity (w/mk), Cp = specific heat (J/kgk), ρ = density (kg/m^3)

some values for Pr are: 0.16-0.7 for mixtures of noble gases with hydrogen, 0.7-0.8 for air and many other gases, around 7 for water (at 20 degree Celsius), between 100 to 40,000 for engine oil and around 1*1025 for earth's mantle. For mercury, conduction of heat is very effective in comparison to convection and diffusivity (thermal) is dominant.

The thickness of momentum and thermal boundary layers are controlled by Prandtl number. when Pr is small, it means heat diffuses very quickly compared to the velocity (momentum).

1.6.3. Nusselt number

The Nusselt number is the ratio of convective to conductive heat transfer across the boundary. The conductive component is measured under the same setting as the heat convection but with a (hypothetically) stagnant fluid.

Nu_L=convective heat transfer/conductive heat transfer =hL/k

L = characteristic length, k = thermal conductivity and h = heat transfer coefficient. If Nu=1(unity) infers that convection and conduction are of similar degree, is feature of "slug flow" or laminar flow. The large value of Nusselt number infers more prominent convection, with turbulent flow in the range of 100-1000.

1.6.4. Grashof number

The Grashof number (Gr) is the ratio of the buoyancy to viscous force acting on a fluid. Usually encountered where natural convection is involved.

$Gr = g\beta\Delta T\rho^2 D^3/\upsilon^2$

where g, β, ΔT are the coefficient of gravitational force, volumetric thermal expansion coefficient and temperature difference, respectively. At higher Grashof numbers the boundary layer is turbulent; at lower Grashof numbers, the boundary layer is laminar.

1.6.5. Richardson number

The ratio of potential to kinetic energy and if the Richardson number is < unity, buoyancy is insignificant in the flow. If it is > unit , buoyancy is dominant (in the sense that there is inadequate kinetic energy). If the Richardson number is of the order unity, then the flow is likely to be buoyancy-driven, The Richardson number in this context is defined as

$Ri = Gr/Re^2$

Ri=0: Forced convection, $Ri=\infty$: Free convection, Ri >: Aiding flow mixed convection (heated cylinder, i.e., where the buoyancy acts in the same direction as the flow)

Ri < 0: opposing flow mixed convection (cooled cylinder, i.e., where the buoyancy and the flow are in opposite directions)

1.5.6. Strouhal number

It is well known that the non-dimensional frequency of oscillation in lift is termed as Strouhal number ($St=f\ L/U_\infty$) and the vortex shedding frequency f is measured from the variation of lift coefficient. 'L' is the characteristic length and 'v' is the velocity of the fluid this characteristic length is the amplitude of oscillation.

Chapter 2: Literature review

Most of the researchers have focused on the investigation of flow around normal geometry like a circular cylinder through experimental, theoretical and numerical approaches. A set of theoretical and review articles are now available for the flow of Newtonian fluids past circular cylinders **[2 - 6]**. Now a days the flow and transfer of heat around non-circular cross-sections have received considerable attention. **Goujon-Durand et al. [7]** experimentally investigated the shedding of vortex formation and envelope of peak to peak amplitude velocity oscillations on the rear side of the cylinder. An impulsively started laminar flow around an expanded trapezoidal cylinder with the range of Reynolds number $25<Re<1000$ was studied by **Lee[8]**. In this work four main flow regimes has been carried out, according to it, on all the faces of the cylinder the flows are predominantly attached also the flow circulation develops at the rear end of the cylinder. There is major flow separation from the principle edge of the cylinder. The variation of Strouhal number (St) from a tapered trapezoidal cylinder was studied numerically by **Chung and Kang [9]** It was observed that both the Reynolds number and height ratio effects the Strouhal number from cylinders. The Strouhal number increases as the ratio of heights from the square section decreases. It was also observed that Strouhal number shows variation with the height ratio and for Re=100,150,and 200. The numerical results obtained in the study of **Kahawita and Wang [1]** has been confirmed by experimental behaviour reported by **Goujon-Durand et al. [7]** at lower Reynolds number, about $Re/Re_c < 2$. For Re=65, i.e. $Re \approx 1.55Re_c$, the present numerical results indicate that the amplitude maximum occurs at a location of about 4.25b, **Goujon-Durand et al. [7]** reported the corresponding location 4b or 4.5b. It was also observed that for a fixed trapezoidal height 'b' in the axial direction the value of Strouhal number is almost independent of the value of the small base width 'a' at lower Re. In a recent study, **Dhiman and Hasan [10]** investigated the 2-D unconfined streamline profiles and transfer of heat across a long bluff body for Re range 1-150 and Pr=0.7 (air). Between Re=5 and 6, It was found that the beginning of flow separation takes place. For Re=46 and 47 there is the switch from a steady to a periodic unsteady regime. The correlation is also provided for the Nu (average) in the steady regime.

It is also apparent that very limited work is currently available on the flow and heat transfer around an expanded trapezoidal bluff body. In another study **Lee [11]**, numerically

investigated the early stages of laminar flow for the range $25 \leq Re \leq 1000$ around the bluff body. For $Re < 25$, the starting flow develops with no visible flow separation. After some time, the flow gets detached from the back face of the cylinder, and forms eddies within a recirculation zone. As the Reynolds number increases the point of stagnation moves fast in the downstream direction. **Chen et al. [12]** investigated two dimensional flow around cylinder (expanded trapezoidal) and also porous in nature. The results are presented with flow configuration for Darcy number 10^{-2}-10^{-3}, porosity from 0.4-0.8 and Re 20-200. when $Da \leq 10^{-4}$; the Darcy number becomes smaller at large Darcy number, the fluctuation-amplitude of drag coefficient decreases, the Reynolds number has to be higher before the vortex shedding phenomena occurs. Recently, **Dhiman and Ghosh [13]** study the steady and periodic forced convection flow and transfer of heat past a long bluff body for Re=1-150. The re-circulation length increases as Re increases in the steady regime ($1 \leq Re \leq 47$). The switch from steady to unsteady regime occurs between Re=47 and 48. There is approximately 146% and 141% enhancement in the transfer of heat as compared to tapered and square cylinders. Further correlations of drag, Nu average, wake length and Strouhal number with Reynolds numbers have also been established. The value of average Nusselt number for the expanded cylinder increases monotonically with the increase in Reynolds number in both steady and time depended regimes.

Venugopal et al. [14] carried out experimental investigations on the vortex flow meter with the differential wall pressure measurement method at high Reynolds number of the order of 10^5. Three different blockages (14%, 24% and 30%) were considered in this study and it was demonstrated that the vortex flow meter comprising of a trapezoidal cross-section is one of the major contributors in the field of flow metering. The vortex shedding from different bluff bodies has been numerically studied by **El-Wahed et al. [15]** at high Reynolds numbers. The results indicate how the shape of the object can influence the nature of the shed vortices. It was observed that the T shaped shedder produce vortices of large size. The vortices are mainly be concentrated near the centerline of the meter body behind the cylinder and by this one can get the good signal by a sensor placed in this region. It is observed that small vortices are formed at both sides of the front face of the shedder

Similarly, **Singha and Balachandra [16]** investigated experimentally the structure statistics in the recirculation region of a sharp-edged bluff body of trapezoidal shape placed upright in a shallow channel and concluded that the wakes formed behind a bluff body are found

to contain a considerable number of coherent structures. For von Karman vortex street investigation, flow visualization supported by image processing acts as a useful tool as reported by **Pankanin and Kulińczak [17]**. The obtained results confirmed the findings of the simulation. The slit in the bluff body takes a part of the stagnation region as an information medium of generated vortices. The phenomenon is strongly dependent on the bluff body geometry. **Schewe and Larsen [18]** showed the effects of Reynolds number in the flow around a bluff bridge deck trapezoidal and affirmed that an significant practical inference of this assumption is that parameters such as St, C_L and C_D may be obtained from low speed wind tunnel model tests and applied directly to the model. It was concluded that bodies with sharp edged cross-section such as bridge box girders may have distinct Reynolds number effect. Also, **Schewe [19]** works on the results of experiments carried out for the broad range of Re (10^4<Re<10^7) in the wind tunnel under high pressure, using different bodies along with trapezoidal-shaped bridge element. It was observed that by shifting the value of Re led to striking changes in the force coefficient and St number. Reynolds number effects can have radical consequences on the unsteady behavior. The examination of the pressure probe properties as the sensor in the vortex flow meter which is tapered trapezoidal in shape has been carried out by **Sun et al. [20]**. The pressure sensor are functional to improve the design of duct-wall differential pressure method in flow measurement and also gives in-depth understanding about the measurement of differential pressure. A bluff body flow meter arrangement of this cross-section also finds its use in controlling air pollution produced by internal combustion engines as stated by **Rodely et al. [21]**. **Sun [22]** has made an analysis of the on the performance and design of the converging-diverging vortex flow meter. It is found that the lower measurement limit can be obtained through the converging-diverging structure, compared to conventional vortex flow meters. **Steggel and Rockliff [23]** demonstrated effects of varying side ratio L/D (0.4≤L/D≤) for the flow around rectangles under both uniform and oscillatory flow. A good consensus with experimentation is found for Re ≥ 500 also the calculated Strouhal number is higher than experimental. It was also observed that Cd increases, with decreasing L/D at Re=200. Frequency of vortex shedding is determined here by **Venugopal et al. [24]**. The numerical simulations reveal that the K-ε RNG model predicts the Strouhal number near to the experimental results than the other models. The effects of sampling rate, tap location and blockage effects, are explored. Among all the bodies the trapezoidal body is found to be finest among all.

It can thus be concluded from the above discussion that no information is currently available on the effects of Prandtl numbers and on the onset of shift from a steady to a unsteady regime for the forced convection heat transfer from a confined trapezoidal cylinder. Therefore, the main objectives of the present work are to investigate the effects of Prandtl numbers and to determine the shift from a steady to a unsteady regime for different values of Re and β. Heat transfer correlations have also been established in terms of the Colburn j_h factor. Furthermore, the present study is the natural extension of our recent work [13] for Re=1-40 and β=0.125-0.50, albeit at a fixed Pr of 0.71 (air).

CHAPTER-3: Formulation and numerical methodology

3.1. Problem description

Figure 1 shows geometrical configuration of 2-D incompressible and laminar flow over a long tapered trapezoidal bar having upstream face width and axial cylinder height b each, and downstream face width a (=0.5b) [5, 13]. The domain is considered to be confined by employing wall confinements (β) ranging from 12.5% to 50%, where β is defined as b/H. The long tapered trapezoidal bar is maintained at a constant temperature of T_w^* and exposed to a fluid stream of average velocity U_∞ and temperature $T_\infty (< T_w^*)$ at the inlet. After a thorough investigation (section 3), the distance from the inlet to the anterior face of the cylinder (X_u) is set as 12b and the downstream distance between the posterior face of the trapezoidal and the exit plane (X_d) is taken as 20b, with the total length of computational domain (L) of 33b in the *x*- direction. The detailed procedure to fix these dimensions is given in section 3 after specifying the governing equations and boundary conditions.

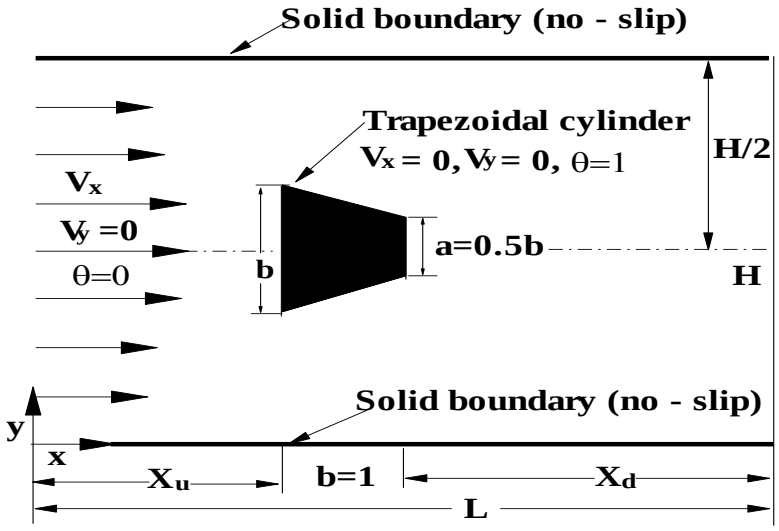

Figure 1*: Sketch of the flow around a confined tapered trapezoidal body in a channel*

The equations used in their dimensionless form for the present system can be written as follows

Continuity equation

$$\frac{\partial V_x}{\partial x}+\frac{\partial V_y}{\partial y}=0 \tag{1}$$

x - Momentum equation

$$\frac{\partial V_x}{\partial t}+\frac{\partial (V_x V_x)}{\partial x}+\frac{\partial (V_y V_x)}{\partial y}=-\frac{\partial p}{\partial x}+\frac{1}{\mathrm{Re}}\left(\frac{\partial^2 V_x}{\partial x^2}+\frac{\partial^2 V_x}{\partial y^2}\right) \tag{2}$$

y - Momentum equation

$$\frac{\partial V_y}{\partial t}+\frac{\partial (V_x V_y)}{\partial x}+\frac{\partial (V_y V_y)}{\partial y}=-\frac{\partial p}{\partial y}+\frac{1}{\mathrm{Re}}\left(\frac{\partial^2 V_y}{\partial x^2}+\frac{\partial^2 V_y}{\partial y^2}\right) \tag{3}$$

Energy equation

$$\frac{\partial \theta}{\partial t}+\frac{\partial (V_x \theta)}{\partial x}+\frac{\partial (V_y \theta)}{\partial y}=\frac{1}{\mathrm{Re}\,\mathrm{Pr}}\left(\frac{\partial^2 \theta}{\partial x^2}+\frac{\partial^2 \theta}{\partial y^2}\right) \tag{4}$$

In this study, the properties like (density, viscosity and thermal conductivity) of the flowing fluid are considered to be temperature independent and the viscous effects are also negligible such that the present situation are applicable, where the difference in temperature is not too large.

The non-dimensional form of B.C's for the confined flow and transfer of heat across a cylinder can be written as

- *At inlet:* $\mathrm{V_x}=1.5[1-(|1-2\beta y|)^2]\ (0\le \mathrm{y}\le \mathrm{H/b};\beta=\mathrm{b/H}), \mathrm{V_y}=0 \text{ and } \theta=0$
- *At above and below channel walls:* $V_x=0, V_y=0$ (no-slip) and $\partial\theta/\partial y=0$ (adiabatic)
- *On the face of a cylinder:* $\mathrm{V_x}=0, \mathrm{V_y}=0$, (no-slip) and $\theta=1$
- *At the exit of channel:* $\partial V_x/\partial x=0,\ \partial V_y/\partial x=0$ and $\partial\theta/\partial x=0$

3.2. Numerical details and choices of numerical parameters

The governing equations (1 - 4) along with above mentioned B.C's (boundary conditions) are solved by using a CFD solver Ansys Fluent [26]. The velocity profile (fully developed) at the channel inlet is incorporated by using user defined functions available in Ansys Fluent [26] and 0.01is to be set as dimensionless time step [10, 25]. The resulting algebraic equations are solved by Gauss-Siedel iterative method in conjunction with AMG solver. The equations like continuity (mass), component (Navier-Stokes) and of energy are used in the order of 10^{-10} each

in the steady regime and of 10^{-20} each in the time-periodic regime. In this study, all the simulations are carried out in an Intel Xeon^{TM} (2.40 GHz) workstation of the Department of Chemical Engineering, IIT Roorkee.

3.2.1 Grid dependence study

The grid structure is generated here is shown in Figure 2. Briefly, the computational grid structure has both uniformity and non-uniformity in grid distributions with the finest size of 0.002b (near the cylinder and just near the upper and lower walls of the channel) and the coarsest grid size of 0.4b with 100 points (CVs) on each side of a trapezoidal cylinder. The grid optimization study is carried out for the value of the blockage ratio of 50% by using three grids (42044 cells, 67040 cells and 92084 cells with 75CVs, 100CVs and 125CVs prescribed on each side of the trapezoidal obstacle, respectively) at the largest value of the Reynolds number of 40 fixed in this work for the Prandtl number of 0.71. The percentage differences between the total drag coefficients are found to be < 1.4% for both the grid sizes of 67040 cells and 92084 cells with respect to the results of drag coefficient at the grid size of 42044 cells. The resultant %age deviation in the values of Nusselt numbers are found to be < 0.70% for both the size of 67040 cells and 92084 cells, respectively. Thus, the grid size of 67040 cells is used for β = 50%. Thus for β = 12.5% and 25%, the size of grid 101280 cells and 75600 cells are found sufficient.

3.2.2 Domain optimization study

The distance from inlet to front face of cylinder is optimized by carrying out the tests for two values of upstream distances of 12b and 17b and for the two extreme vales of β i,e 12.5% and 50%. The relative %age deviations in the values of total C_D and average cylinder Nu (average) are found to be negligible and about 0.02% respectively for β = 12.5% for the Pr of 0.71 (Table 1). Further, the same upstream test has been carried out for the Pr of 100 which shows the negligible variation in the values of C_D and Nu.

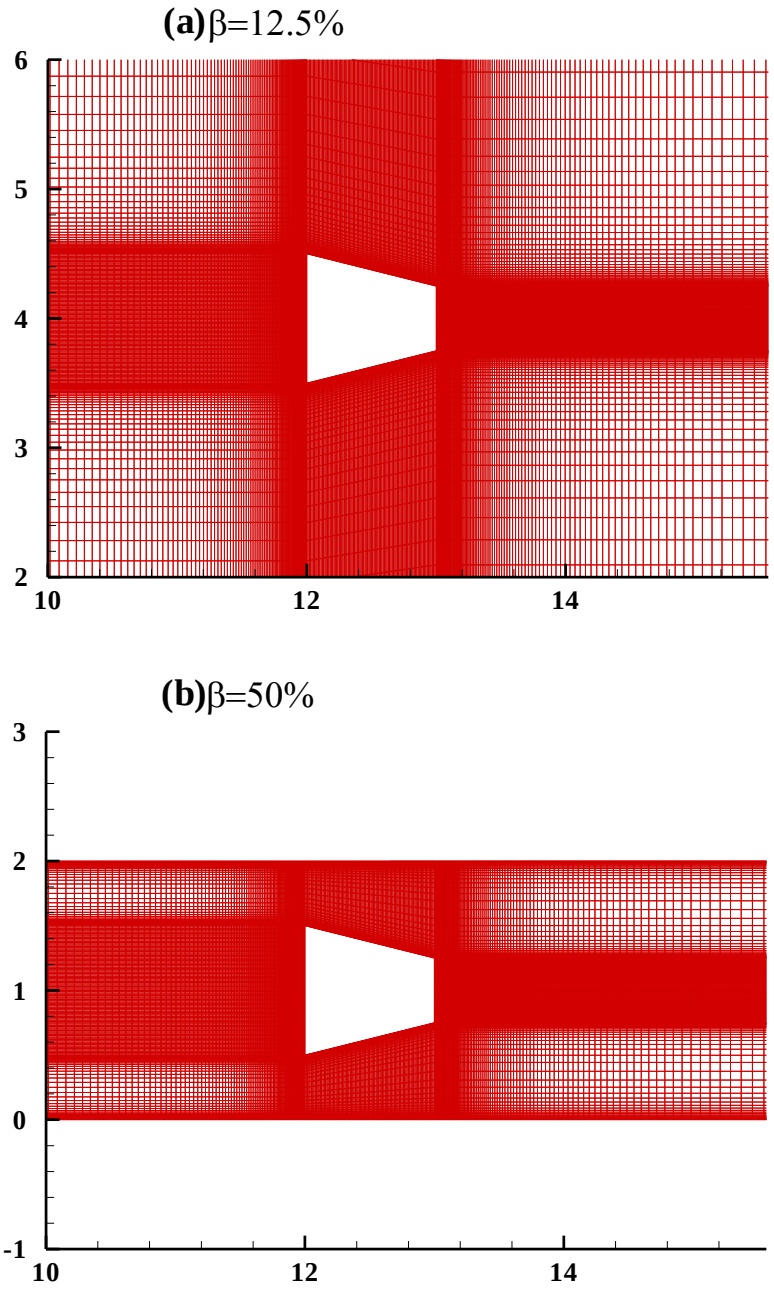

Figure2: *Grid structures around a confined cylinder for different* β

For the same conditions mentioned above, upstream dependence test has been carried out for the β of 50%, as shown in Table 1. The relative percentage difference in the values of total C_D and N_u are negligible and about 0.02% for Pr=0.71, and for Pr=100 the corresponding differences in the C_D and N_u are negligible. Therefore, the distance of 12b is fixed from inlet to front surface of cylinder.

***Table 1**: Effects of upstream distances (X_u) for β of 12.5% and 50% for Re=1 and for Pr of 0.71 and 100*

β=12.5%	Pr=0.71	X_d=20, X_u=17	X_d=20, X_u=12	% deviation
	C_D	33.4919	33.4919	Negligible
	$\bar{N}u$	0.8085	0.8084	0.02
	Pr=100			
	C_D	33.4919	33.4919	Negligible
	$\bar{N}u$	3.8340	3.8340	Negligible
β=50%	Pr=0.71			
	C_D	260.1585	260.1585	Negligible
	$\bar{N}u$	0.3518	0.3519	0.02
	Pr=100			
	C_D	260.1585	260.1585	Negligible
	$\bar{N}u$	6.1631	6.1361	Negligible

Similarly, the downstream dependence is checked for the two extreme values of 20b and 25b of downstream distances at Reynolds number equal to 40. The relative %age deviation in the values of overall C_D and Nu (average) are found to be < 0.003% and 0.002% respectively for the β of 12.5% and for Pr. as 0.71, as shown in Table 2. It is further observed under the same conditions but for the Prandtl number of 100, the relative percentage difference in C_D and Nu is 0.002% and 0.001% respectively. The downstream dependency has also been carried out for the blockage ratio of 50% as shown in Table 2. The relative percentage differences in the values of overall C_D and cylinder $\bar{N}u$ are 0.05% and 0.01% and for Pr=0.71. Further, the deviation in the values of C_D and $\bar{N}u$ are found negligible for a Prandtl number equal to 100. Therefore, the

distance of 20b is found sufficient from rear side of cylinder up-to the exit, for the generation of results. Furthermore, Table 2 presents the downstream effect for the Re of 100 and for the β of 50% because of the fact that the shift from a steady to a unsteady regime for this blockage ratio occurs between Re=91 to 92. The percentage differences of C_D and $\bar{N}u$ for the downstream distances of 25b and 20b are found about 0.03% and 0.31% respectively. Thus, the downstream distance of 20b is again found adequate for further simulations.

***Table 2**: Effects of downstream distances (X_d) for β of 12.5% and 50% and for Pr of 0.71 and 100*

	Pr=0.71	X_d=25, X_u=12	X_d=20, X_u=12	% deviation
β=12.5%,Re=40	C_D	3.4944	3.4943	0.002
	$\bar{N}u$	2.9114	2.9114	0.001
	St	0.1757	0.1760	0.15
	Pr=100			
	C_D	3.4944	3.49433	0.002
	$\bar{N}u$	17.2540	17.2541	0.001
	St	0.1770	0.1760	0.56
β=50%, Re=40	Pr=0.71			
	C_D	9.8209	9.8160	0.05
	$\bar{N}u$	3.9092	3.90958	0.01
	Pr=100			
	C_D	9.8209	9.8209	Negligible
	$\bar{N}u$	19.2651	19.2651	Negligible
β=50%, Re=100	Pr=0.71			
	C_D	8.3861	8.3889	0.03
	$\bar{N}u$	5.2178	5.2018	0.31
	St	0.5319	0.5319	Negligible

CHAPTER-4: Results and discussions

It is also worthwhile to mention here that in oil and chemical related industries the value of Pr up to about 100 are commonly observed, particularly in the processing of organic liquids like glycols, olive oil and glycerol's, etc. [27 - 29]. In addition, calculations are carried out to determine the shift from a steady to a unsteady regime for all the blockage ratios considered. The various engineering parameters such as drag coefficient, local and average Nusselt numbers and the Colburn heat transfer factor are calculated and discussed. The representative streamline and isotherm profiles are provided to recognize the thermal and flow structures around the tapered cylinder under consideration. The results thus obtained after numerical simulation have been compared with results available in the literature in the next section. Simple empirical equations relating the physical parameters under study with the Reynolds number have been derived. The applicability range of these correlation is fine.

4.1. Validation

The comparison of the current study findings is first made with the results of ref. [9] on the long cylinder for the Re of 100 and 150 (Table 3) by considering the same domain. An outstanding concordance is found between the present values and that given in ref. [9]. For example, the maximum deviations in St. no are found to be < 1.0% and 2.2% for Re = 100 and 150. Further, because of the non-availability of experimental results in the literature, Table 4 provides the similarity of C_D and $\bar{N}u$ for the transfer of heat and flow for the highest Reynolds number (Re=40), and for the blockage ratio of 25% in the steady flow regime. Exceptional concurrence can be seen between the present results and the values reported in literature [30 - 33] and the maximum deviation can be seen of the order of 0.10% for drag coefficient and 0.25% for Nusselt number.

***Table 3**:Validation of Strouhal number (St) with Chung and Kang [9]*

Source	Strouhal number
Re=100	
Current work	0.14
Ref.[9]	0.138
Re=150	
Current work	0.15
Ref.[9]	0.149

***Table 4**: Drag coefficient and Nusselt number(average) validation with literature values at Re=40 for β=25%*

source	(C_D)	($\overline{Nu}$)
Present work	1.7039	4.6701
Bharti et al.[30]	1.7034	-
Rao et al.[31]	1.7054	-
Bijjam and Dhiman [32]	1.7039	-
Bharti et al.[33]	-	4.6593

4.2. Flow patterns

Extensive details on the flow of air (i.e. at Pr=0.71) around a trapezoidal cylinder in a channel can be found in our recent study [25], it is not replicated here. The flow pattern is represented by streamline contours around the long tapered trapezoidal cylinder in steady regime. Streamline contours are a group of constant velocity lines in the domain of present study which help in identifying the nature of flow (i,e steady or unsteady). Briefly, as the Reynolds number increases the flow separates at the trailing edge of the cylinder as shown in Fig. 3. The distance from just near the back side of the object to the point of connection for the closed near wake on the axis of symmetry is defined as wake length, an important flow parameter. It has been observed that for a fixed β, the recirculation region increases as there is increase in Re. This nature is found to be similar to that of the confined flow across the square [28, 29, 34], triangular [35, 36] and circular [30 - 32] cylinders. For the fixed value of Reynolds number, the size of recirculation region decreases with an increase in blockage ratio. In prolongation of preceding efforts of Dhiman et al. [25], Fig. 4 shows the change in the wake length for the tapered cylinder with Re in the steady regime along with the values found in ref. [28]. The recirculation length is found higher for square cylinder at Re ≤ 10 for β=12.5% and 25% as shown in Figures. 2a and 2b; however, for Re>10, a contrary tendency of the wake length is observed with the increasing difference in the increasing value of wake length for the two obstacles.

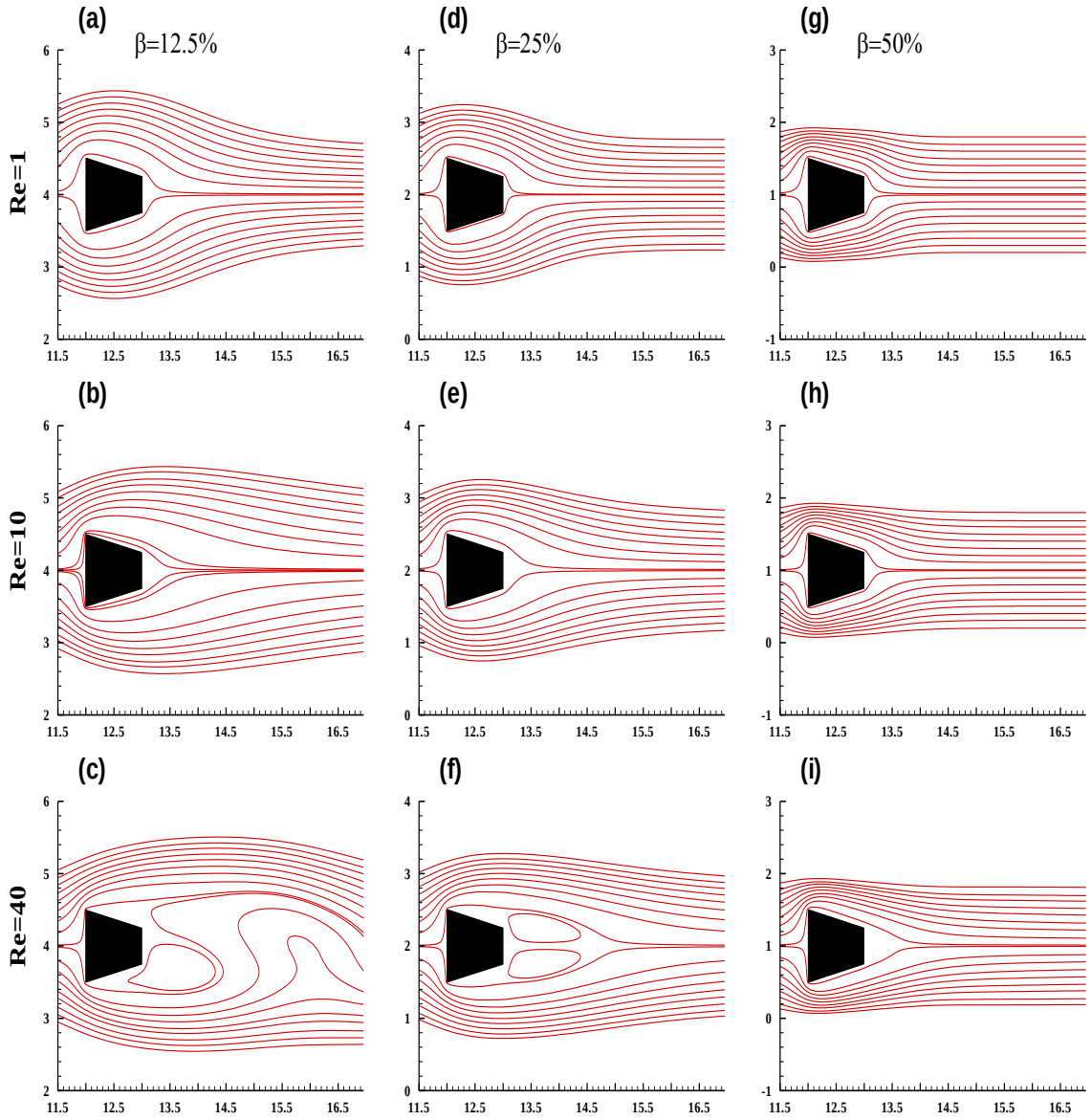

***Figure3**: Streamline contours for Re=1,10 and 40 for different β*

.

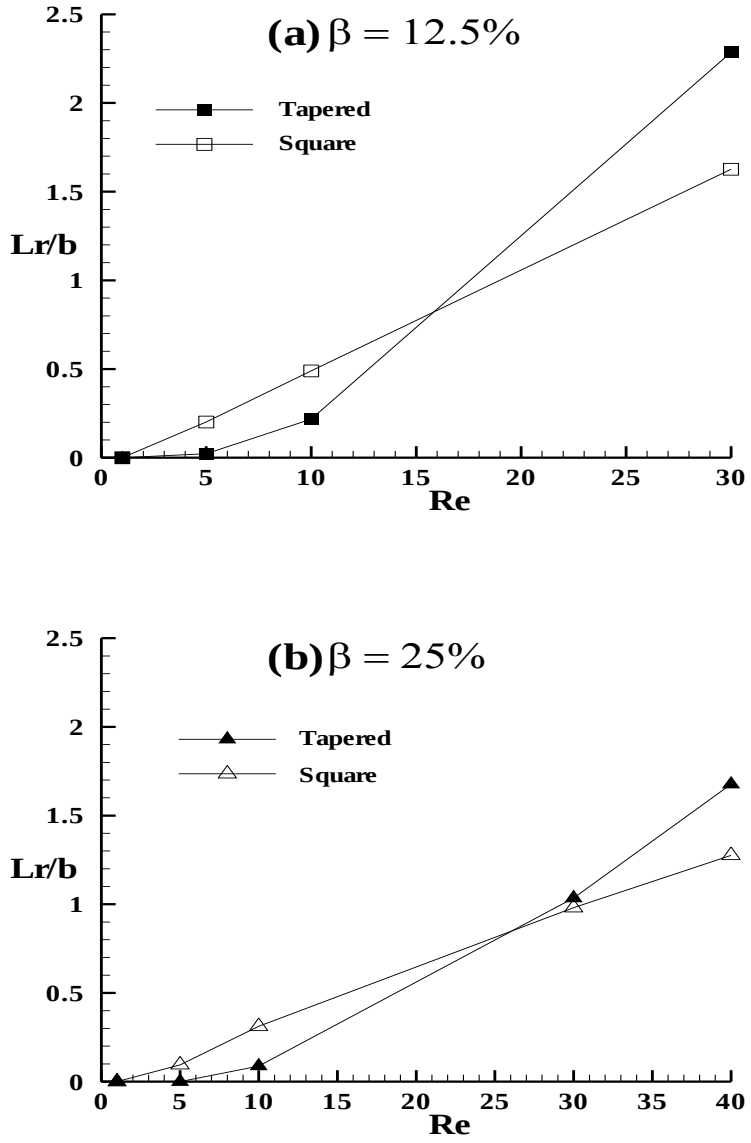

Figure 4*: Change in recirculation length with Reynolds number along with values of cylinder [28] for different β in the steady regime.*

This abnormality is due to the fact that the separation of flow in the present case of tapered trapezoidal cylinder takes place from top and bottom surfaces along with the rear corners. However, in case of a square cylinder, flow separation occurs only from the rear corners.

4.3. Transition from a steady to time-periodic flow

One of the major objectives of this study is to the find the critical Reynolds number (i.e. the shift from a steady to a unsteady regime), the values of the physical output parameters like drag and lift coefficients, and Nusselt number are monitored and plotted with respect to time.

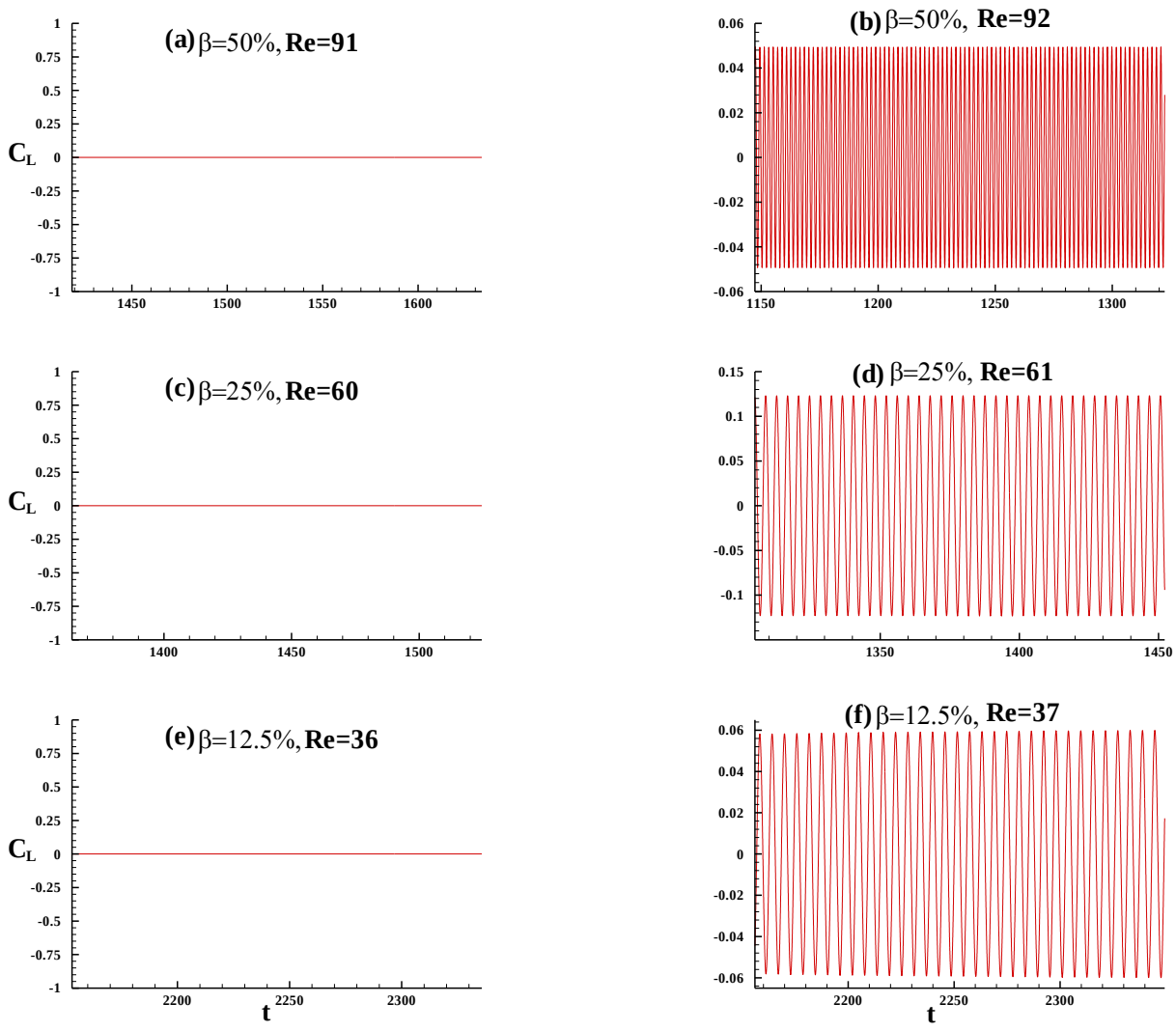

Figure 5*: The time history of the lift coefficient showing the shift from a steady to a unsteady regime at various values of β*

For instance, the lift coefficient (C_L) is illustrated at various values of Re and β in Figures. 3a-3f. After scrutinizing the streamline contours Figure 3 and lift coefficient pattern, it is concluded that for the β of 0.125, 0.25 and 0.50, the transition occurs at Reynolds numbers of 37, 61 and 92 respectively as shown in Figure. 5. The critical Reynolds number increases with the increase in blockage ratio (β) and it has been confirmed by carrying out the time dependent numerical simulations in the full computational domain. This is consistent with the findings of Srikanth et al. [35] and Turki et al. [36], respectively.

4.4. Thermal patterns

The effects of Reynolds number on the thermal structures around an bluff body of are investigated for Re in the range of (1-40) in steady regime at Pr=0.71-100. Figures 4 and 5 present the representative isotherms close to the long trapezoidal obstacle at Pr (=0.71, 50 and 100) for the β of 12.5%, 25% and 50%, for the extreme values of Re=1 and 40 respectively. Obviously, the thermal effects are more evident at low values of Reynolds and Prandtl numbers as viscous effects are more prevailing in the steady regime or one can conclude that the conduction is more dominant at this juncture. As the value of Pr is progressively increased from 0.71 to 100, the thermal boundary layer thickness decreases, for the set values of β and Re. On the other hand, the isotherms are highly disturbed by the adiabatic walls, e.g. as shown in Figures. 4d and 4g for β=50% and 25% at Re=1 and Pr=0.71. The reduction of temperature field increases with the rise in the Prandtl number at different blockage ratios as and can also be seen in Figs. 6 and 7. It is also observed that for the blockage ratio of 12.5% the wavering effect increases with the rise in Pr. number because of time-periodic nature found at Re=40. Similar to the confined square [28, 29, 34], triangular [35] and circular [33] cylinders in a channel, the highest concentration of isotherms is observed on the front end of the tapered bluff body which is quite apparent from the thermal patterns (Figs. 6 and 7). It therefore results in high transfer of heat from the front face of the cylinder in comparison to the other faces of the cylinder.

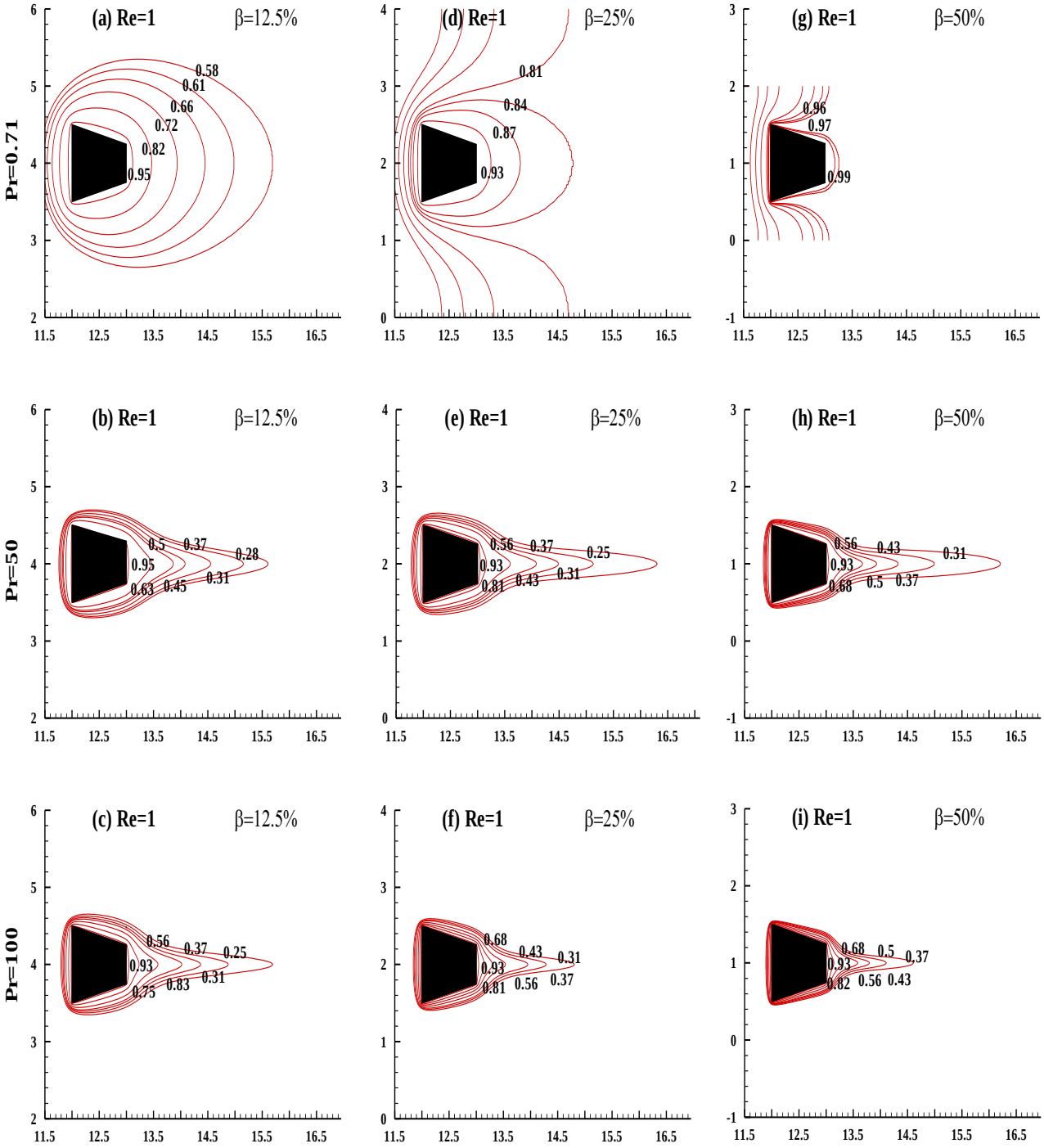

***Figure 6**: Isotherms for constant cylinder temperature for Reynolds number (Re=1) and Pr=0.71, 50 and 100 at different β.*

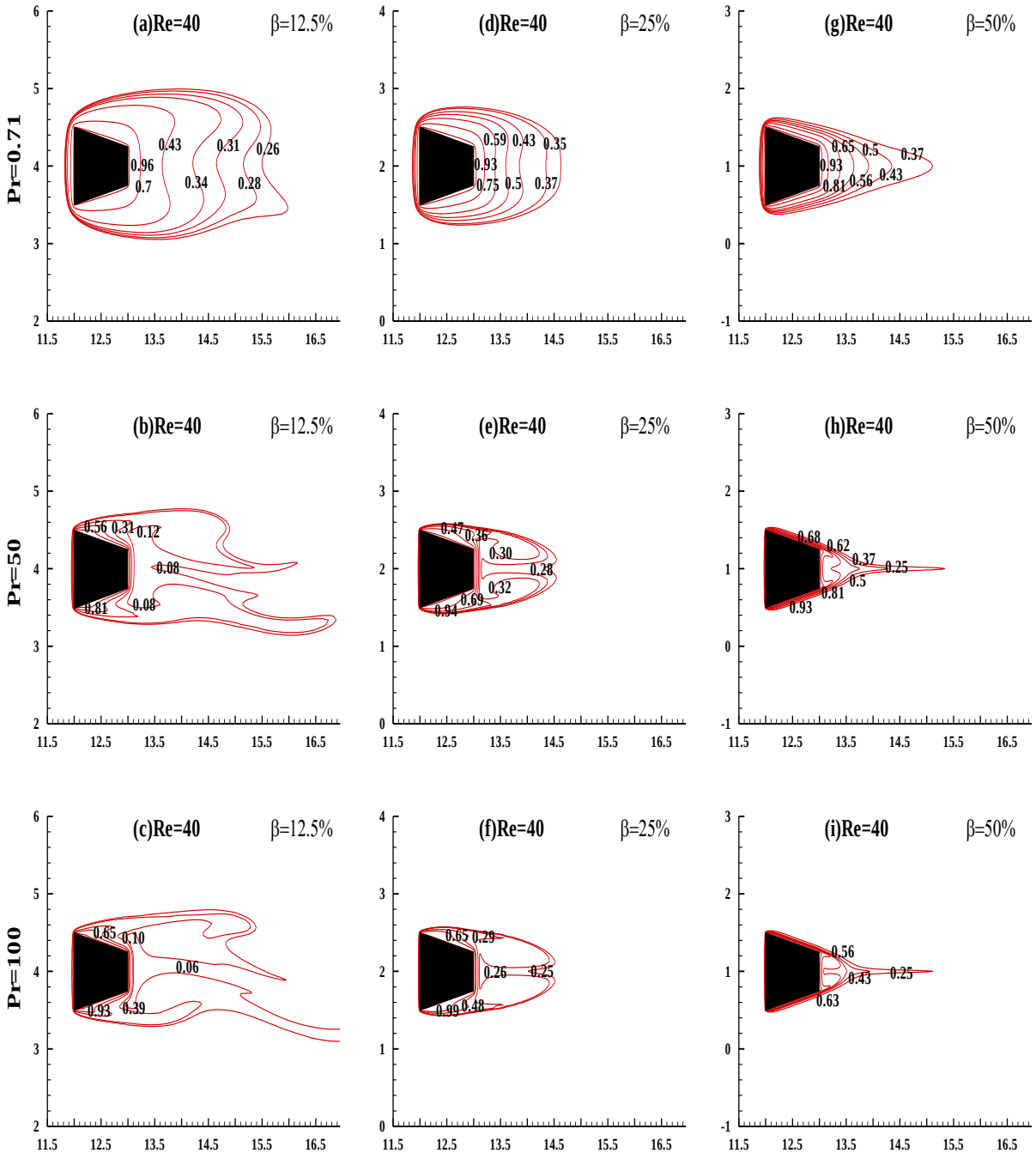

***Figure 7**: Isotherms for constant cylinder temperature for Re=40 and Pr=0.71, 50 and 100 at different blockage ratios*

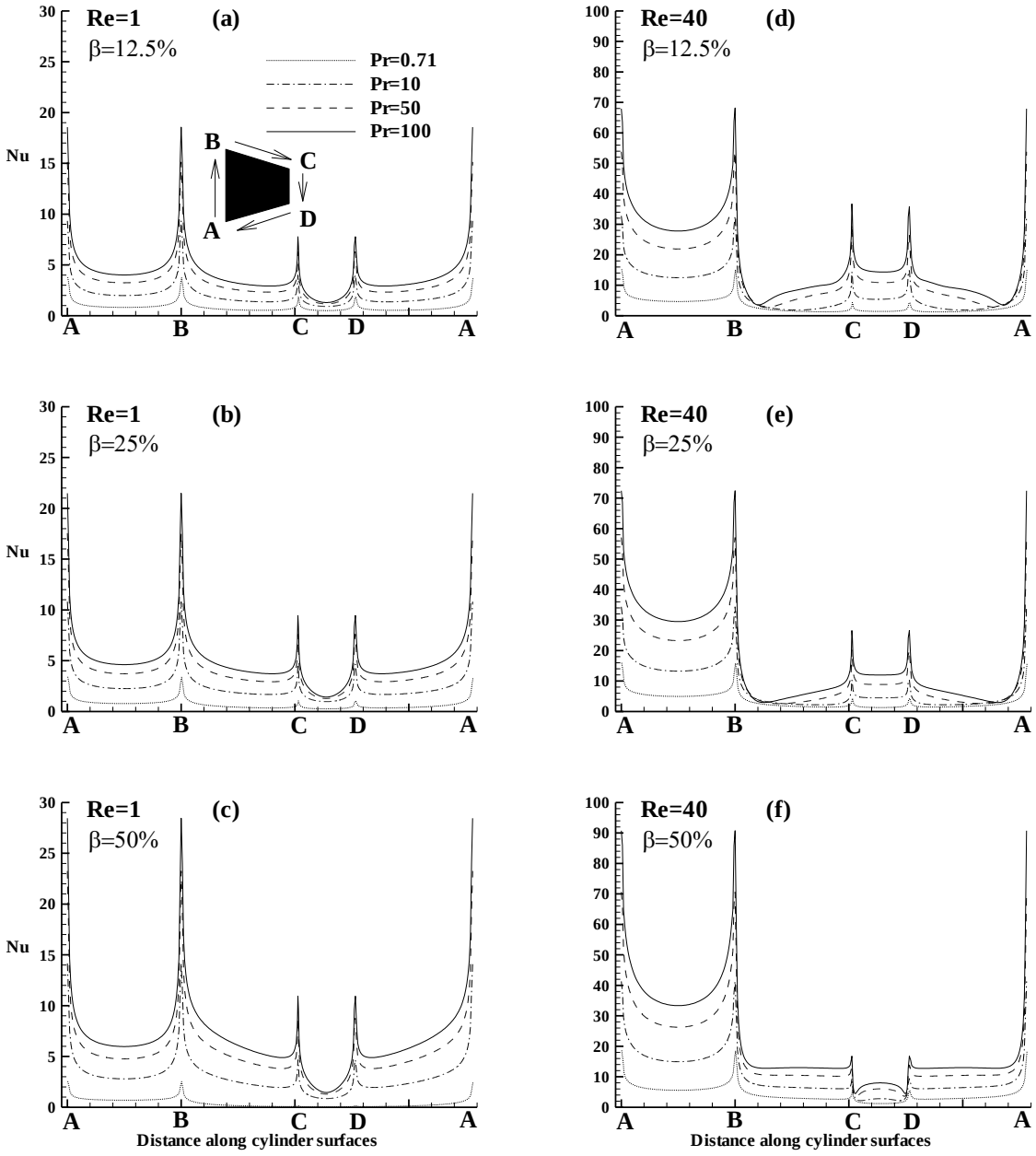

Figure 8*: Nusselt number (local) variation along the four faces of the 2-D cylinder for Re=1-40 at different β and Pr.*

4.5. Local Nusselt number

Figure 8 shows the influence of β on the change of the Nu (local) along the cylinder surfaces of the tapered trapezoidal cylinder at Re=1 and Re=40 for Pr equal to 0.71, 10, 50 and 100. It is evident from the plots that for the particular β, the Nu increases with the rise in the values of Re and/or Pr. The Nu (local) also rises due to the blockage ratio stems mostly from the sharp change in the temperature gradients. Moreover, due to the high temperature gradient normal to the face of the body, each corner of the trapezoidal cylinder shows high value of Nu. The Nusselt number (local) increases in the direction of the corners (A or B) on the front surface of the tapered trapezoidal cylinder as there is the highest concentration of isotherms at this face thereby resulting in high transfer of heat from the front surface similar to what has been observed in a confined square cylinder [28, 29, 34]. The value of Nu (local) decreases on the top and bottom face and then increases piercingly toward the posterior corners at point 'C' and 'D' shown in figure 8 of the cylinder. Overall, the change of the Nusselt number (local) around the trapezoidal cylinder surfaces is found to be symmetric for top and bottom halves of the channel in the steady regime. Because the temperature field is found to be unsteady in nature at β=12.5% for Re=40, the sample of instantaneous variation of local Nusselt number at different Pr is shown in Fig. 8d.

4.6. Average Nusselt number

The cylinder $\bar{N}u$ (average) of the tapered trapezoidal cylinder is obtained by averaging the average Nusselt number over the each face of the object. Figure 9 shows the variation of the Nusselt number (average) for the tapered trapezoidal cylinder as a function of Reynolds number and blockage ratio for Prandtl numbers ranging from 0.71-100. Parts a-d of Fig. 9 show that the $\bar{N}u$ (average) enhance with the increase of Reynolds number due to increased movement of fluid same what has been observed in unconfined tapered [10] and expanded [13] trapezoidal cylinders. It is also seen that the $\bar{N}u$ (average) for the trapezoidal cylinder increases with increasing Prandtl numbers for all blockages ratios (Figs. 9a-9d). Particularly, the average cylinder Nusselt number increases with increasing blockage ratio for the Reynolds number range $5<Re\leq40$ and Prandtl number of 0.71 (Fig.9a), however the average cylinder Nusselt number decreases with blockage ratio for the Reynolds number of unity and the mixed trend is observed

for Reynolds number of 5 [25] as the main reason for this trend is the prominent effect of conduction at Pr=0.71, while this trend is not obeyed at higher Prandtl numbers. The behaviour of average Nusselt number at Pr>0.71 in Figs. 9b - 9d is somewhat similar to that of Pr=0.71 (Fig. 9a) for Re>5 but it was also found that average Nusselt number shows a quantum jump at Re=40 for β=12.5%, and the reason for this remarkable behaviour is the time-periodic nature at Re =40. Further, Fig. 10 shows the distinction of the average Nusselt of the tapered trapezoidal cylinder with that of a square cylinder [16] for the blockage ratios of 12.5% and 25% and for Prandtl numbers in the range 0.71-100 in the steady flow regime.

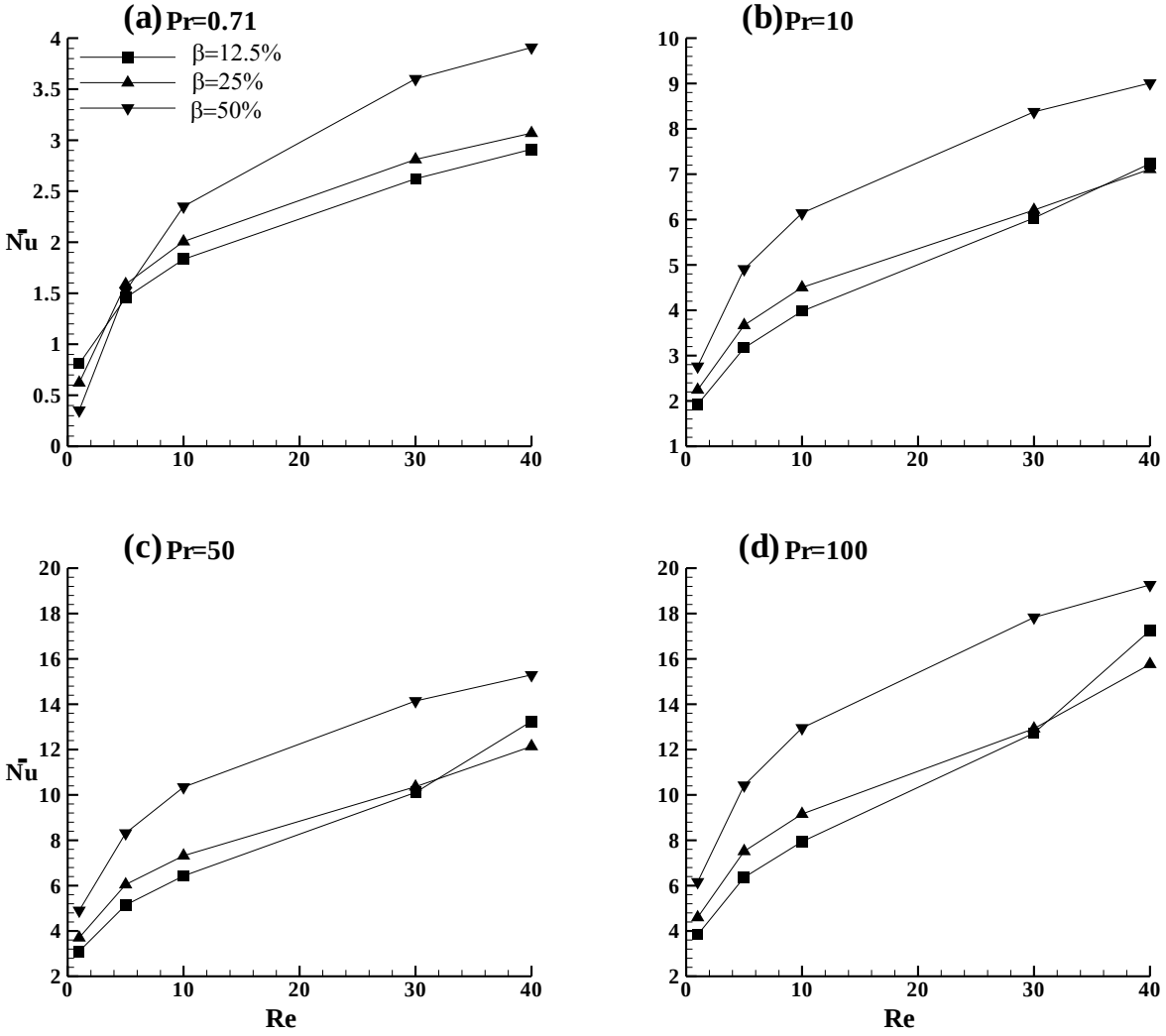

Figure 9*: Change of the cylinder Nusselt number (average) with Re and blockage ratio for different Prandtl number of the tapered trapezoidal cylinder*

It is found from Fig. 10a for β=0.125 that the $\bar{N}u$ (average) of the cylinder is greater than the square cylinder. However, Fig. 10b depicts as the β increases from 12.5% to 25% the $\bar{N}u$ (average) of the square cylinder starts to exceed from the Nusselt number (average) of tapered one for higher Prandtl numbers (Pr≥10). For instance, it is clear from the figure that if Re>10 the average Nusselt number of the square cylinder starts to exceed the average Nusselt number of the tapered cylinder, e.g. Pr=10, 50 and 100. The main reason behind this behaviour is, as the Reynolds number increases there is early boundary layer separation in tapered trapezoidal body as compared to square cylinder. The boundary layer detaches at the rear end of the cylinder (square) while as for tapered cylinder the separation takes place from top and bottom surfaces along with the rear corners, which results in the reduction in heat transfer for the tapered cylinder [10, 25]. The $\bar{N}u$ (average) of cylinder under investigation was found on the higher side as compared with that of the cylinder [25] due to belated flow detachment for the range of Re≤10.

It can also be concluded from Figs. 10a and 10b that as the Re and Pr increase there is the enhancement in transfer of heat rate for the tapered cylinder as compared with the square cylinder. The percentage enhancements of the average Nusselt number for a tapered trapezoidal bluff body with respect to a square cylinder in both the confinements of 12.5% and 25% have been calculated as $\left|(\bar{N}u - \bar{N}u_{Square})/\bar{N}u_{Square}\right|\times 100$ and represented in Table 5. The maximum enhancement in heat transfer for a tapered trapezoidal bluff body with respect to a square cylinder is found to be approximately 31% and approximately 45% for β of 12.5% and 25% respectively for the Pr of 0.71 and Re=1. It is also observed that the percentage heat transfer enhancement goes on decreasing as the Prandtl number and/or Reynolds number increase(s) for both the blockages and for all Prandtl numbers as the reason is already discussed in the above paragraph.

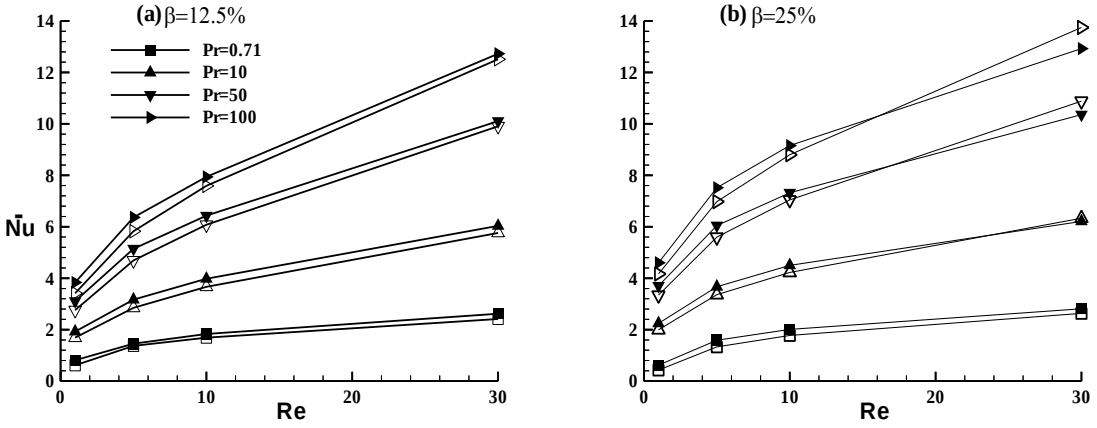

Figure 10: Average Nusselt numbers for the tapered trapezoidal cylinder (solid symbols) and the Square cylinder (open symbols) [28] as a function of Pr and Re for β=12.5% and 25% in the steady regime

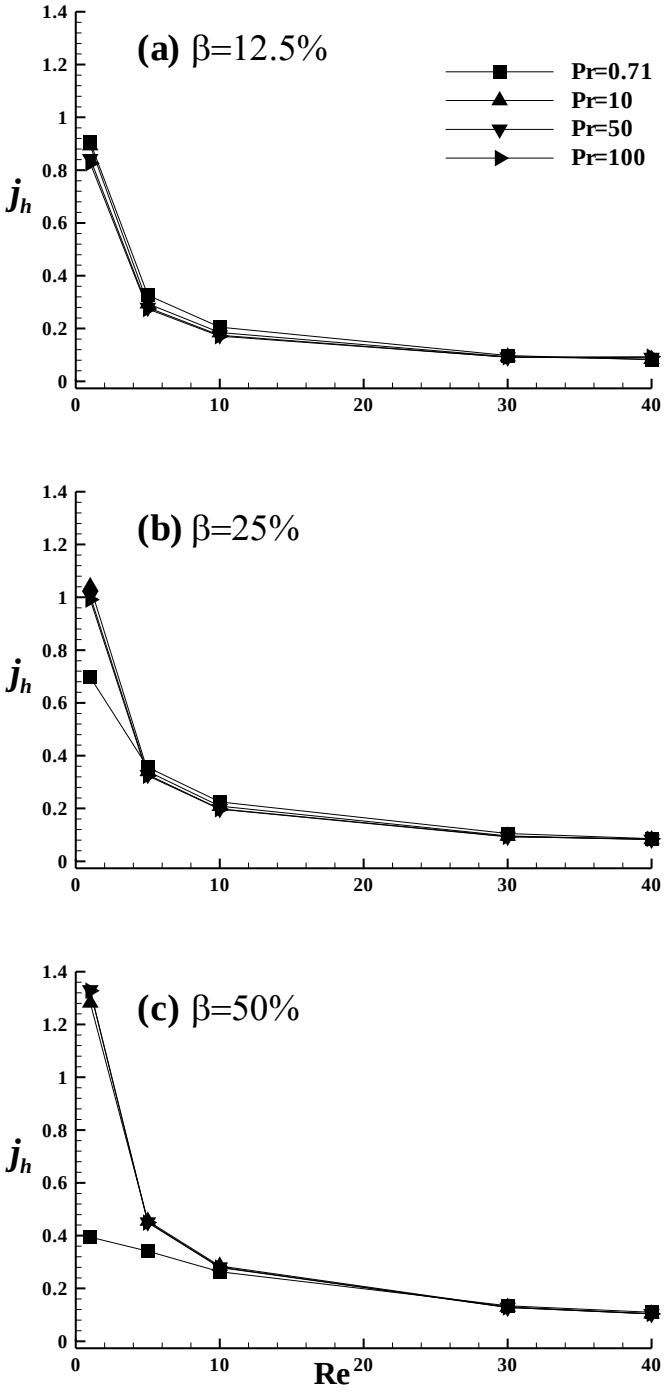

Figure 11*: The Colburn j_h factor as a function of Re at various Pr and blockage ratios*

Table5*:* Percentage enhancement for the tapered trapezoidal cylinder with respect to the cylinder [28]

	$\overline{Nu}$		β=12.5%	$\overline{Nu}$		β=25%
Re(Pr=0.71)	Tapered obstacle	Square obstacle	% Enhancement	Tapered obstacle	Square obstacle	% Enhancement
1	0.8087	0.6160	31.28	0.6223	0.4305	44.54
5	1.4554	1.3667	6.49	1.5880	1.3305	19.35
10	1.8329	1.6877	8.60	2.0066	1.7751	13.04
30	2.6216	2.4159	8.51	2.8110	2.6345	6.70
40	2.9113	2.6947	8.04	3.0688	2.9276	4.82
Re(Pr=10)						
1	1.9244	1.6877	14.03	2.2438	1.9927	12.60
5	3.1691	2.8472	11.31	3.6695	3.3580	9.28
10	3.9791	3.6669	8.51	4.5018	4.2217	6.63
30	6.0352	5.7608	4.76	6.2100	6.3317	1.92
Re(Pr=50)						
1	3.1065	2.7576	12.65	3.7041	3.3434	10.79
5	5.1451	4.6905	9.69	6.0466	5.5979	8.04
10	6.4304	6.0776	5.81	7.3195	7.0439	3.91
30	10.1084	9.9066	2.04	10.3619	10.8858	4.81
Re(Pr=100)						
1	3.8339	3.4144	12.29	4.5993	4.1667	10.38
5	6.3642	5.8284	9.19	7.5153	6.9781	7.70
10	7.9405	7.5904	4.61	9.1571	8.7999	4.06
30	12.7250	12.5112	1.71	12.9257	13.7462	5.97

4.7. Coulburn heat transfer factor

Further, the average Nusselt number varies approximately linearly with respect to Reynolds and Prandtl numbers and blockage ratio; it is suitable to show a relationship that represent transfer of heat by simple expressions in terms of the Colburn factor (j_h)

$j_h = \overline{Nu} / (\mathrm{Re}\ \mathrm{Pr}^{1/3})$

Figures 9a-9c show the depicts results in terms of j_h factor at three different values of β. The j_h values resultant to the values of Pr are seen to overlap for particular value of β for the Re in the range of $1 \leq Re \leq 40$. Some deviations at $Re < 5$ for β=25% and at $Re \leq 10$ for β=50% and for Pr=0.71 can be observed. Table 6 shows the correlations established for different range of Prandtl numbers as well as for different blockage ratios. These correlations have the average deviations of about 3.65%, 2.85% and 5.80% for β=50%, 25% and 12.5% respectively for the Reynolds number range $1 \leq Re \leq 40$ and Prandtl number range $10 \leq Pr \leq 100$. However, the maximum deviations are about 7.30%, 5.30% and 10.40% for β=0.50, 0.25 and 0.125 respectively. It is also important to mention here that the average deviation for β=12.5% is about 4.35% for the range $1 \leq Re \leq 30$ and $10 \leq Pr \leq 100$ as at Re=40 the flow shows time-periodic behavior, and 15-45 points are used for generating these correlations. The correlation derived for Pr=0.71 is somewhat different because of prominent conduction here and as such the trend in Figs. 11b and 11c is unusual at lower Prandtl and Reynolds numbers .

Table 6: *Error analysis for the generalized correlations of the Colburn j_h factor*

B	Prandtl number	Generalized Correlation	Average % deviation	Maximum % deviation	R^2
50%	0.71	$j_h=0.48Re^{-0.35}$	-	-	0.867
	10,50,100	$j_h=1.3Re^{-0.69}$	3.63	7.30	
25%	0.71	$j_h=0.78Re^{-0.57}$	-	-	0.980
	10,50,100	$j_h=0.99Re^{-0.68}$	2.85	5.30	
12.5%	0.71	$j_h=0.92Re^{-0.65}$	-	-	0.999
	10,50,100	$j_h=0.80Re^{-0.63}$	5.80 and 4.32*	10.40	

* If excluding the point (at Re=40) where the flow shows time-periodic behaviour

CHAPTER 5: Conclusions and Recommendations

conclusions

Two-dimensional investigation across the cylinder of tapered trapezoidal cross section in an confined steady regimes are explored for Re=1-40 and Pr=0.71-100

- The effects of Prandtl numbers ($0.71 \leq Pr \leq 100$) and blockage ratios (β=12.5%, 25% and 50%) on characteristics of heat transfer of a tapered trapezoidal cylinder confined in a channel have been carried out at low Reynolds numbers.

- The critical Reynolds number is calculated and it exists between Re = (36 and 37), (60 and 61) and (91 and 92) for β of 12.5%, 25% and 50% respectively, also as the blockage ratio increases the critical Reynolds number increases.

- The maximum enhancement in heat transfer for a tapered trapezoidal bluff body with respect to a square cylinder is found to be approximately 31% and 45% for the blockages of 12.5% and 25% respectively for Pr=0.71 and Re=1.

- Finally, the Colburn heat transfer j_h factor correlations have been developed for the preceding range of conditions

Recommendations

Following points can be carried out as the future work in this field:

- This work depicts 2-D phenomena only and for more accurate results simulations can be carried out in 3-D pattern .

- The same study can be carried out for non-Newtonian fluids.

- The same problem can be studied under aiding buoyancy conditions.

References

[1] R. Kahawita, P. Wang, Numerical Simulation of the wake flow behind trapezoidal bluff bodies, Comp. Fluids 31 (2002) 99-112.

[2] M.M. Zdravkovich, Flow around Circular Cylinders: Fundamentals, Oxford University Press, New York, 1997.

[3] M.M. Zdravkovich, Flow around Circular Cylinders: Applications, Oxford University Press, New York, 2003.

[4] V.T. Morgan, The overall convective heat transfer from smooth circular cylinders, Adv. Heat Transfer 11 (1975) 199 - 264.

[5] C. Norberg, Fluctuating lift on a circular cylinder: review and new measurements, J. Fluid Structures 17 (2003) 57 - 96.

[6] R.P. Chhabra, Fluid flow and heat transfer from circular and noncircular cylinders submerged in non-Newtonian liquids, Adv. Heat Transfer 43 (2011) 289-417.

[7] S. Goujon-Durand, K. Renffer, J.E. Wesfreid, Downstream evolution of the Benard von Karman instability**,** Phys. Rev. E 50 (1994) 308 - 313.

[8] T.S. Lee, Early stages of an impulsively started unsteady laminar flow past tapered trapezoidal cylinders, Int. J. Numer. Meth. Fluids 26 (1998) 1181–1203.

[9] Y.J. Chung, S.H. Kang, Laminar vortex shedding from a trapezoidal cylinder with different height ratios, Phys. Fluids **12** (2000) 1251 – 1254.

[10] A.K. Dhiman, M. Hasan, Flow and heat transfer over a trapezoidal cylinder: steady and unsteady regimes, Asia Pacific J. Chem. Eng. 8 (2013) 433-446.

[11] T.S. Lee, Numerical study of early stages of an impulsively started unsteady laminar flow past expanded trapezoidal cylinders, Int. J. Numer. Meth. Heat Fluid Flow 8 (1998) 934-955.

[12] X.B. Chen, P. Yu, S.H. Winoto, H.T. low, Numerical analysis for the flow past a porous trapezoidal cylinder based on the stress jump interfacial conditions, Int. J. Numer. Meth. Heat Fluid Flow 19 (2009) 223-241.

[13] A.K. Dhiman, R. Ghosh, Computer simulation of momentum and heat transfer across an expanded trapezoidal bluff body, Int. J. Heat Mass Transfer 59 (2013) 338 - 352.

[14] A.Venugopal, A. Agrawal, S.V. Prabhu, Influence of blockage and upstream disturbances on the performance of a vortex flowmeter with a trapezoidal bluff body, Meas. 43 (2010) 603-616.

[15] A.K. El-Wahed, M. Johnson, J.L. Sproston, Numerical study of vortex shedding from different shaped bluff bodies, Flow Meas. Instrm. 4 (1993) 233-240.

[16] A. Singha, R. Balachandra, Coherent structure statistics in the wake of a sharp edged bluff body placed vertically in a shallow channel, Fluid Dyn. Res. 43 (2011) 055504-055526.

[17] G.L. Pankanin, A. Kulińczak, Determination of vortex convection velocity with application of flow visualization and image processing, Metrol. Meas. Syst. 18 (2011) 361-370.

[18] G. Schewe, A. Larsen, Reynolds number effects in the flow around a bluff bridge deck cross section, J. Wind Engg. 74 - 76 (1998) 829 - 838

[19] G. Schewe, Reynolds-number effects in flow around more-or-less bluff, J. Wind Engg. 89 (2001) 1267 - 1289

[20] Z. Sun, H. Zhang, J. Zhou, Investigation of the pressure probe properties as the sensor in the vortex flow meter, Sensors and Actuators A: Physical 136 (2007) 646 - 655

[21] A. Rodely, T.J. Fussel, Bluff body flow meter arrangement for use in controlling air pollution produced by internal combustion engines, US Patent: 3722275, 1973

[22] Z. Sun, Design and performance of the converging-diverging vortex flow meter, Metrol. Meas. Syst. 18 (2011) 129 - 136

[23] N. Steggel, N. Rockiff, simulations on the effects of body shape on lock in characteristics in pulsating flow by the discrete vortex method, J. Wind Eng. Ind. Aerodyn. 69-71 (1997) 317-321

[24] A.Venugopal, A. Agrawal, S.V. Prabhu, Influence of blockage and shape of a bluff body on the performance of vortex flowmeter with wall pressure measurement, Meas. 44 (2011) 954-964.

[25] A.K. Dhiman, S. Verma, R. Ghosh, Laminar momentum and heat transfer in a channel with a built-in tapered trapezoidal bluff body, Heat Transfer-Asian Research, 2013, In press.

[26] ANSYS User Manual, Ansys Inc., 2009.

[27] A.K. Dhiman, R.P. Chhabra, A. Sharma, V. Eswaran, Effects of Reynolds and Prandtl numbers on heat transfer across a square cylinder in steady flow regime, Numer. Heat Transfer A 49 (2006) 717-731

[28] A.K. Dhiman, R.P. Chhabra, V. Eswaran, Flow and heat transfer across a confined square cylinder in the steady flow regime: Effect of Peclet number**,** Int. J. Heat Mass Transfer 48 (2005) 4598–4614.

[29] A.K. Dhiman, R.P. Chhabra, V. Eswaran, Steady mixed convection across a confined square cylinder, Int. Comm. Heat Mass Transfer 35 (2008) 47-55.

[30] R.P. Bharti, R.P. Chhabra, V. Eswaran, Two-dimensional steady Poiseuille flow of power-law fluids across a circular cylinder in a plane confined channel: wall effects and drag coefficients, Ind. Eng. Chem. Res. 46 (2007) 3820-3840.

[31] M.K Rao, A.K. Sahu, R.P. Chhabra, Effect of confinement on power-law fluid flow past a circular cylinder, Polymer Eng. Sci. 51(2011) 2045-2065.

[32] S.Bijjam, A.K. Dhiman, CFD analysis of two-dimensional non-Newtonian power-law flow across a circular cylinder confined in a channel, Chem. Eng. Comm. 199 (2012) 767-785.

[33] R.P. Bharti, R.P. Chhabra, V. Eswaran, Effect of blockage on heat transfer from a cylinder to power law liquids, Chem. Eng. Sci. 62 (2007) 4729-4741.

[34] A.K. Dhiman, N. Sharma, S. Kumar, Wall effects on the cross-buoyancy around a square cylinder in the steady regime, Brazilian J. Chem. Eng. 29 (2012) 253 -264.

[35] S. Srikanth, A.K. Dhiman, S. Bijjam, Confined flow and heat transfer across a triangular cylinder in a channel, Int. J. Therm. Sci. 49 (2010) 2191 - 2200.

[36] S. Turki, H. Abbassi, S.B. Nasrallah, Effect of the blockage ratio on the flow in a channel with a built-in square cylinder, Comp. Mech. 33 (2003) 22-29.